

# Modeling Accelerated Pick-up Ion Distributions at an Interplanetary Shock

Errol J. Summerlin & Matthew G. Baring

*Department of Physics and Astronomy, MS-108, Rice University, P. O. Box 1892,  
Houston, TX 77251-1892, USA*  
Emails: [xerex@rice.edu](mailto:xerex@rice.edu), [baring@rice.edu](mailto:baring@rice.edu)

---

## Abstract

The acceleration of interstellar pick-up ions as well as solar wind species has been observed at a multitude of interplanetary (IP) shocks by different spacecraft. The efficiency of injection of the pick-up ion component differs from that of the solar wind, and is expected to be strongly enhanced at highly oblique and quasi-perpendicular shock events, in accord with inferences from *in situ* observations. This paper explores theoretical modeling of the phase space distributions of accelerated ions obtained by the Ulysses mission for the Day 292, 1991 shock associated with a corotating interaction region, encountered before Ulysses' fly-by of Jupiter. A Monte Carlo simulation is used to model the acceleration process, adapting a technique that has been successfully tested on earlier IP shocks possessing minimal pick-up ion presence. Phase space distributions from the simulation technique for various low mass ions are compared with SWICS and HI-SCALE data to deduce values of a "turbulence parameter" that controls the efficiency of injection, and the degree of cross-field diffusion. Acceptable fits are obtained for the  $H^+$  and  $He^+$  populations using standard prescriptions for the pick-up ion distribution;  $He^{++}$  spectral data was only fit well for scenarios very close to the Bohm diffusion limit. It is also found that the simulation successfully accounts for the observation of energetic protons farther upstream of the forward shock than lower energy pick-up protons, using the same turbulence parameter that is required to achieve reasonable spectral fits.

*Key words:* Interplanetary shocks, Co-rotating interaction regions, Ulysses mission, Diffusive shock acceleration, Shock turbulence

---

## 1 Introduction

Particle acceleration at collisionless shocks is believed to be a common phenomenon in space plasmas in a diversity of environments, ranging from the inner heliosphere to the central regions of distant galaxies. In the heliosphere, evidence to support the belief that such a mechanism can efficiently produce non-thermal particles includes direct measurements of accelerated populations in various energy ranges at the Earth's bow shock (e.g. Scholer et al. 1980; Möbius et al. 1987; Gosling et al. 1989) and interplanetary shocks (for the pre-Ulysses era see, for example, Sarris and Van Allen 1974; Gosling et al. 1981; Decker, Pesses and Krimigis, 1981; Tan et al. 1988). The motivations for developing theories of shock acceleration are therefore obvious, and a variety of approaches have emerged. One possible means for the generation of non-thermal particles is the Fermi mechanism, often called diffusive shock acceleration; it is this process that is the focus of this paper.

There are various approaches to modelling diffusive shock acceleration. Among these are convection-diffusion differential equation approaches (e.g. Kang and Jones 1995), and the kinematic Monte Carlo technique of Ellison and Jones (e.g., see Jones and Ellison, 1991, and references therein), which describes the injection and acceleration of particles from thermal energies; both of these can address spectral and hydrodynamic properties. This latter simulational approach is the central tool for the analysis here, and is ideally suited to the interpretation of the modest time-resolution shock data acquired by Ulysses. Hybrid and full plasma codes (e.g. Quest 1988; Burgess 1989, Winske et al. 1990; Trattner and Scholer 1991; Giacalone, Burgess and Schwartz 1992; Liewer, Goldstein, and Omidi 1993; Kucharek and Scholer 1995) provide contrasting probes of shock environs, with an emphasis primarily on plasma structure and wave properties in the environs of shocks.

Comparisons of predictions from theoretical models with observed phase-space distribution data are informative probes. The first detailed theory/data comparison along these lines was performed by Ellison, Möbius and Paschmann (1990) in the case of the quasi-parallel portion of the Earth's bow shock, comparing predictions of the Monte Carlo method with particle distributions of protons,  $He^{++}$  and a  $C$ ,  $N$  and  $O$  ion mix obtained by the AMPTE experiment. The agreement between model predictions and data was impressive. Ellison, Möbius and Paschmann (1990) concluded that a successful fit was possible only in the non-linear acceleration regime, when the dynamic effects of the accelerated particles are crucial to the determination of the shock structure. Since this pioneering work, successful comparisons of other theoretical techniques with data from the Earth's bow shock have been performed. These include the hybrid plasma simulations of Trattner and Scholer (1991) and Giacalone et al. (1993), and solutions to the convection-diffusion equation (Kang

and Jones 1995), both of which have yielded good agreement with both the bow shock data and the Monte Carlo technique (Ellison et al. 1993).

Such a comparison between theory and experiment was extended to the domain of interplanetary shocks in the work of Baring, Ogilvie, Ellison and Forsyth (1997, hereafter BOEF97; see also Kang & Jones 1997, for application of their convection-diffusion equation technique). In this development, impressive agreement was found between the Monte Carlo predictions and spectral data obtained by the Solar Wind Ion Composition Spectrometer (SWICS) aboard Ulysses, in the case of two shocks observed early in the Ulysses mission. Such agreement was possible only with the assumption of strong particle scattering (i.e. near the Bohm diffusion limit) in the highly oblique candidate shocks. For a third shock, detected a month later, the comparison failed, with significant differences arising in the 500-800 km/sec range of the phase space distribution. BOEF97 attributed this discrepancy to the omission of pick-up ions from the model: such an extra component would be expected to provide a substantial contribution to the accelerated population in this particular event.

This paper addresses the role of pick-up ions in such shocks via modeling the accelerated population for the specific interplanetary shock observed on day 292 of 1991, detected by the SWICS and HI-SCALE instruments aboard the Ulysses spacecraft at around 4.5 AU, as reported in Gloeckler et al. (1994). Phase space distributions from the simulations are compared with SWICS and HI-SCALE data, yielding acceptable fits for the  $H^+$  and  $He^{++}$  populations, using standard prescriptions for the injected pick-up ion distribution, by adjusting a single turbulence parameter  $\eta$ . Using this same  $\eta$ , the simulation results also successfully account for the observation of energetic protons farther upstream of the forward shock than lower energy pick-up protons, since a rigidity-dependent diffusion is used in the models.

## 2 The Monte Carlo Simulation Technique

The Monte Carlo simulation technique used here has been invoked in previous applications to shocks in the heliosphere, as discussed above, and is extensively described in a number of papers (Ellison, Jones, & Eichler 1981; Ellison, Jones & Reynolds 1990; Jones & Ellison 1991; Baring, Ellison & Jones 1994; Ellison, Baring, & Jones 1996). It follows closely Bell's (1978) test particle approach to diffusive acceleration. Particles are injected upstream and allowed to convect into the shock, meanwhile diffusing in space so as to effect multiple shock crossings, and thereby gain energy through the shock drift and Fermi processes. For the interplanetary shock that is the focus of this paper, throughout  $u_1$  and  $u_2$  shall denote the upstream and downstream flow speed in the shock rest frame, respectively.

The particles gyrate in a laminar electromagnetic field. Their trajectories are obtained by solving a fully relativistic Lorentz force equation in the shock rest frame, in which there is, in general, a  $\mathbf{u} \times \mathbf{B}$  electric field in addition to the magnetic field. The effects of magnetic turbulence are modeled by scattering these ions in the rest frame of the local fluid flow. These collisions, effectively mimicking diffusive transport instigated by Alfvén waves, are assumed to be elastic in the local fluid frame, an assumption that is valid so long as the flow speed far exceeds the Alfvén velocity. Otherwise, the scattering centers are not anchored in the fluid frame, and the collisions are inelastic, thereby introducing significant second-order Fermi (stochastic) acceleration. For interplanetary shocks in general, and in particular for the Day 292, 1991 shock considered here, the elastic scattering assumption is somewhat violated due to a low shock Alfvénic Mach number. Yet the stochastic acceleration contribution is expected to be relatively small, perhaps at most of the order of 25%, so its inclusion is deferred to later work.

The simulation can routinely model either large-angle or small-angle scattering. In this paper, large-angle scattering is employed, motivated by previous observations (e.g., Hoppe et al. 1981; Balogh et al. 1993) indicating very turbulent fields in IP shocks. Between scatterings, particles are allowed to travel a distance in their local fluid frame that is exponentially distributed about the scattering mean free path  $\lambda$ , with:

$$\lambda = \lambda_0 \left( \frac{r_g}{r_{g1}} \right)^\alpha \propto p^\alpha . \quad (1)$$

Here  $r_g = pc/(qB)$  is the gyroradius of an ion of momentum  $p = mv$ , mass  $m$ , and charge  $q$ . Also  $r_{g1} = mu_{1.x}c/(qB)$  is the gyroradius of an ion with a speed  $v$  equal to the far upstream flow speed normal to the shock plane,  $u_{1.x}$ , where  $x$  denotes the direction normal to the shock plane. The mean free path scale  $\lambda_0$  is set proportional to  $r_{g1}$  with constant of proportionality  $\eta$  such that  $\lambda_0 = \eta r_{g1}$ . Following previous Monte Carlo work, for simplicity we set  $\alpha = 1$ , a specialization that is appropriate for interplanetary plasma shocks (e.g., see Ellison et al. 1990; Mason, Gloeckler & Hovestadt 1983; Giacalone, Burgess & Schwartz 1992 for discussions on the micro-physical expectations for  $\alpha$ ), yet is easily generalizable in the simulation. Since  $\lambda \geq r_g$  for physically meaningful diffusion resulting from gyro-resonant wave-particle interactions, the  $\alpha = 1$  case is also motivated on fundamental grounds.

Cross-field diffusion emerges naturally from the simulation, since at every scattering, the direction of the particle's momentum vector is randomized in the local fluid frame, with the resulting effect that the gyrocenter of a particle is shifted randomly by a distance of the order of one gyroradius in the plane orthogonal to the local field. Transport perpendicular to the field is then governed by a kinetic theory description, so that the ratio of the spa-

tial diffusion coefficients parallel ( $\kappa_{\parallel} = \lambda v/3$ ) and perpendicular ( $\kappa_{\perp}$ ) to the mean magnetic field is given by  $\kappa_{\perp}/\kappa_{\parallel} = 1/(1 + \eta^2)$  (see Forman, Jokipii & Owens 1974; Ellison, Baring & Jones 1995, for detailed expositions). Hence,  $\eta$  couples directly to the amount of cross-field diffusion, and is a measure not only of the frequency of collisions between particles and waves, but also of the level of turbulence present in the system, i.e. is an indicator of  $\langle \delta B/B \rangle$ . Note that  $\eta = 1$  is the Bohm diffusion limit of quasi-isotropic diffusion, presumably corresponding to  $\langle \delta B/B \rangle \sim 1$ . As will become evident in the Section 3, by virtue of its connection to cross-field diffusion,  $\eta$  plays an important role in determining the injection efficiency of low energy particles. We note that other cross-field transport effects such as that incurred by so-called field-line wandering (e.g. see Giacalone & Jokipii 1999) can be incorporated parametrically in the Monte Carlo technique, and will be addressed in future work.

While  $\eta$  and  $\alpha$  serve as parameters here, in principal they can be calculated for a given wave field. However, in practice, precision is limited by *in situ* magnetometer data, and exact determination of 3-dimensional particle diffusion properties from a 1-dimensional field data stream is impossible. Yet insights can be gained by using established theoretical formalism, such as random fluctuation theory (e.g. Jokipii & Coleman 1968), or equivalently quasi-linear diffusion theory (see, e.g., Kulsrud & Pierce 1969; Jones, Birmingham, & Kaiser 1978), to estimate components of the diffusion tensor along and orthogonal to the mean field. These components can be expressed in terms of integrals of components of the power spectral tensor for field fluctuations. Such slab models for turbulence can be extended to consider higher-dimensional field fluctuations (e.g. see Bieber et al. 1994). Guidance for the behavior and values of  $\alpha$  and  $\eta$  can be gleaned from such investigations, and an analysis along these lines to facilitate the interpretation of Ulysses IP shock spectral data will be the subject of future work.

The simulation technique makes no distinction between accelerated particles and thermal ones. Therefore the injection efficiency is determined solely by the a particle's ability to diffuse back upstream after it has encountered the shock for the first time. In the case of the Earth's bow shock (Ellison et al. 1990), this permits the development of a nonlinear model that includes the effects of the accelerated particles on the dynamics of the shock. However, in the relatively weak IP shock considered here, a steep power-law is present, and the poor injection efficiency reduces the number density of energetic particles, eliminating nonlinear hydrodynamic effects. Upstream plasma quantities are input from observational data, as discussed below, and downstream quantities are determined using the full MHD Rankine-Hugoniot relations. The simulation is capable of producing energy spectra/fluxes, and hence phase space distributions, at any location upstream or downstream of the shock and in any reference frame including that of a spacecraft. This makes the simulation ideal for comparison with observational data.

### 3 Modeling the Ulysses Event of Day 292, 1991

Our case study focuses on the forward shock of a CIR encountered by Ulysses on Day 292 of 1991, for which downstream particle distributions were obtained for comparison with data published in Gloeckler et al. (1994). To determine parameters for this shock that are appropriate input for the Monte Carlo simulation, the observational results detailed in Gloeckler et al. (1994) are used along with the data compilations of Balogh et al. (1995), González-Esparza et al. (1996), and Hoang et al. (1995). These sources indicate that the sonic Mach number  $M_s$  of the shock was 2.53, with an unstated uncertainty. This controls the temperature of the thermal solar wind protons, but does receive contributions from electrons and alpha particles. Other parameters include the angle  $\theta_{Bn1} = 50^\circ \pm 11^\circ$  the upstream magnetic field makes with the shock normal,  $B_1 = 0.8$  nT, and magnetic compression ratio  $B_2/B_1 = 2.50 \pm 0.13$ . Here  $B_1$  and  $B_2$  are the *total* magnetic field magnitudes upstream and downstream of the shock, respectively. In addition, the normalization of solar wind distributions was established using  $n_p = 2.0$  cm $^{-3}$  as the solar wind proton density, and  $n_{He} = 4.0 \times 10^{-2}$  cm $^{-3}$  as that for solar wind  $He^{++}$  (within the uncertainties of values listed Table 1 in Gloeckler et al. 1994).

Although fluctuations in the plasma data preclude precise determination of the velocity compression ratio of the shock, Gloeckler et al. inferred a value of  $r = u_1/u_2 = 2.4 \pm 0.3$ . This inference is somewhat inconsistent with the observed  $v^{-5.75}$  power-law behavior of the phase space density at high energies, which suggests a compression ratio nearer 2. The choice of compression ratio is controlled by the shock Mach number  $M_T = M_s M_A / \sqrt{M_s^2 + M_A^2}$ , receiving contributions from sonic and Alfvénic Mach numbers,  $M_s$  and  $M_A$  respectively, which can be written in the form (e.g. Baring et al. 1997):

$$M_s \approx 8.52 \frac{u_{100}}{\sqrt{T_{p4} + T_{e4}}} \quad , \quad M_A \approx 4.58 \frac{u_{100}}{B_{-5}} \sqrt{n_p} \quad , \quad (2)$$

where  $u_{100}$  is the shock speed  $u_{1,x}$  in units of 100 km/sec,  $T_{p4}$  and  $T_{e4}$  are the proton and electron temperatures in units of  $10^4$  K,  $B_{-5}$  is the upstream field strength in units of  $10^{-5}$  Gauss, and  $n_p$  is the proton density in cm $^{-3}$ . Using upstream values of  $T_{e4} = 2.59$  and  $T_{p4} = 1.67$ , as tabulated in Hoang et al. (1995), we find that for  $u_{1,x} = 55$  km/sec,  $M_s \approx 2.5$ . Adding in the magnetic field gives  $M_T \approx 2.1$ . To yield a compression ratio  $r = (\gamma + 1)/[\gamma - 1 + 2/M_T^2] = 2.1$  for adiabatic index  $\gamma = 5/3$ , one must have a slightly lower value of  $M_T \approx 1.85$  (i.e. perhaps higher field). In this paper, we adopted a value of  $r = 2.1$ , which lies within the margin of error of Gloeckler et al.'s inferred value, to generate power-law slopes commensurate with the data. Due to significant observational uncertainties, ranges of parameters are permissible.

In the simulation runs, the temperature  $T_\alpha$  of the  $\alpha$  particles was chosen to be four times that of the solar wind protons. No guidance for this assumed upstream temperature was provided in Gloeckler et al. (1994), nor in the aforementioned Ulysses data compilation papers. However, in the IP shock theory/data comparison of Baring et al. (1997), for the one shock with good measurements of the  $He^{++}$  distribution, namely the 91097 event, the upstream  $\alpha$  particle thermal velocity was comparable to (actually slightly greater) than that of the solar wind protons, implying  $T_\alpha \approx 4T_p$ . Adopting the same temperature ratio  $T_\alpha/T_p$  in this work was motivated by this precedent, and the expectation that the adiabatic expansion of the solar wind from 2.7AU to 4.5AU should roughly preserve the ratios of the temperatures per nucleon for these two ions. Note that the correction to the sonic Mach number in Eq. (2) incurred by solar wind helium is then approximately 4%.

To facilitate transformation of simulation results measured in the shock rest frame to the approximate spacecraft frame, so as to compare directly with Gloeckler et al.'s published distributions, a value for the solar wind plasma speed of  $v_{sw,2} = 393 \pm 12$  km/s was assumed *after* the shock encounter. This identifies the downstream fluid frame. No values for the shock speed were listed in Gloeckler et al. (1994), as is common practice in other expositions (e.g. see Burton et al. 1992; Baring et al. 1997). Hence selection of a value for  $u_{1,x}$  consistent with other data became necessary. From the long-term solar wind radial velocity traces in Figure 2 of González-Esparza et al. (1996) we can set a lower bound on the solar wind speed of  $v_{sw,1} \gtrsim 330$  km/s prior to the shock passage, i.e. upstream. Assuming collinear velocities, i.e. that the solar wind is not deflected by the shock on large scales, we have the speed relations  $u_{1,x} = v_{sh} - v_{sw,1}$  and  $u_{2,x} = v_{sh} - v_{sw,2}$  in addition to  $r = u_{1,x}/u_{2,x}$ , where  $v_{sh}$  is the unknown shock speed in the spacecraft frame. These solve to yield  $u_{1,x} \approx 55$  km/s and  $u_{2,x} \approx 28$  km/s for  $r = 2.1$  for  $v_{sw,1} \sim 360$  km/s; higher values of  $u_{1,x}$  and  $u_{2,x}$  would be realized for smaller choices of  $v_{sw,1}$ .

The other input for the Monte Carlo simulation is that for the incoming pick-up ion distributions. Gloeckler et al. (1994) used a simplified form for these distributions; here we adopt the slightly more developed expression used in Ellison, Jones & Baring (1999) that is modeled on the seminal work of Vasyliunas & Siscoe (1976). This form incorporates the gravitational focusing of interstellar neutrals, the physics of their ionization as a function of distance from the sun (approximately at solar minimum), and adiabatic losses incurred during propagation away from the sun, and is similar in conception to pick-up ion distributions used in le Roux, Potgieter & Ptuskin (1996). Our pick-up ion model therefore provides both the detailed shape and normalization of these superthermal distributions, which are distinctly different for  $H^+$  and  $He^+$ , largely due to the patently different ionization and charge exchange rates for their corresponding interstellar neutrals.

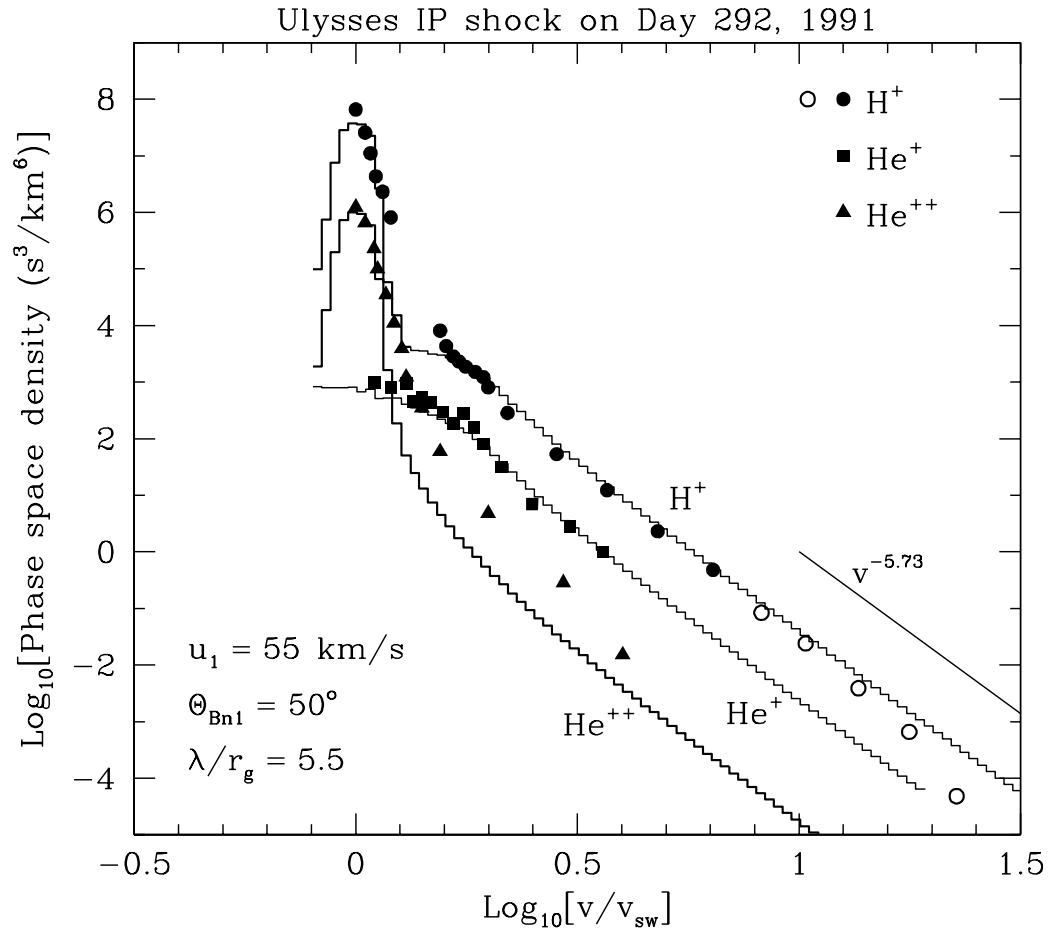


Fig. 1. Phase space velocity distribution functions for data collected by the Ulysses mission for the shock on Day 292 of 1991, specifically for the interval 1991.292.0400-293.0400. The velocity axis is the ratio of the ion speed  $v$ , as measured in the spacecraft frame, to the solar wind speed. The data are for  $H^+$  (filled circles for SWICS data; open circles for HI-SCALE points) solar wind and pickup ions,  $He^+$  (filled triangles) pickup ions, and  $He^{++}$  (filled squares), mostly solar wind ions, and are taken from Gloeckler et al. (1994). The histograms are the corresponding Monte Carlo models of acceleration of these species (heavy weight corresponds to solar wind ions) for  $u_1 = 55 \text{ km/sec}$ , using the optimal choice of plasma shock parameters from Gloeckler et al. (1994) and sources indicated in the text. The model assumed  $\eta = \lambda/r_g = 5.5$  and a shock of compression ratio  $r = 2.1$ , corresponding to diffusive acceleration power-laws of index  $-5.73$ , is indicated.

Downstream distributions for thermal and accelerated ions from the Monte Carlo simulation are compared with SWICS and HI-SCALE measurements taken in the frame of the spacecraft on the downstream side of the Day 292, 1991 shock in Fig. 1. The Ulysses data are those exhibited in Fig. 1 of Gloeckler et al. (1994), and the simulation data are transformed to the spacecraft frame as described above. The solar wind and pick-up ion parameters and

abundances are fairly tightly specified, so that the theoretical model has one largely free parameter, the ratio of the particle mean free path to its gyroradius,  $\eta = \lambda/r_g$ . As noted in Ellison, Baring & Jones (1995) and Baring et al. (1997), the efficiency of acceleration of thermal ions in oblique shocks, i.e. the normalization of the non-thermal power-law, is sensitive to the choice of  $\eta$ , so this parameter was adjusted to obtain a reasonable “fit” to the Ulysses data. Ellison, Jones & Baring (1999) note that for their application to the solar wind termination shock, the efficiency is not as sensitive to  $\eta$  when superthermal pick-up ions enter the problem, a property that we also replicate here. Here, for  $\eta \gtrsim 3$ , the accelerated pick-up ion phase space density is orders of magnitude above that of the thermal ions, for both  $H$  and  $He$ .

In Fig. 1, the theory/data comparison is overall not quite as good as the ones in Baring et al. (1997) for Ulysses IP shock data at around 2–3 AU, where pick-up ions are less of a factor. Yet the fits here do model the accelerated pick-up ions very well, for  $\eta = 5.5$ , a value that is slightly higher than those inferred in the fits of Baring et al. (1997), but is still consistent with a moderate level of field turbulence (i.e. here  $\kappa_\perp/\kappa_\parallel \approx 0.03$ ). Note that since the inferred value of  $\eta = 5.5$  for  $H^+$  and  $He^+$  data is most sensitive to the assumed shock obliquity  $\theta_{Bn1}$  (among other input parameters), the observational uncertainty in  $\theta_{Bn1}$  maps over to an uncertainty of around  $\pm 1.5$  in the value of  $\eta$ .

There are clear differences between the simulation results and the observations. The  $He^{++}$  distribution of thermal solar wind ions appears slightly narrower than the published observations. More notable though is the fact that the accelerated thermal  $He^{++}$  ions are injected somewhat less efficiently in the simulation than in the observations, an inefficiency characteristic of highly oblique shocks that is present also for the *solar wind* protons, though not explicitly displayed in Fig. 1. The efficiency of acceleration of thermal ions could be increased via several means: (i) by lowering the shock obliquity angle  $\theta_{Bn1}$ , for which there is a large observational uncertainty; (ii) by decreasing  $\eta$ , corresponding to increased turbulence, without altering the pick-up ion acceleration efficiencies substantially, and (iii) increasing the temperature of the thermal ions somewhat, though this would reduce the compression ratio and accordingly steepen the non-thermal continuum. However, such parameter adjustments only incur small changes to the widths of the thermal distributions. Trial runs indicate that an agreeable fit can be obtained to the entire  $\alpha$  particle distribution simply by reducing  $\eta$  to  $\eta \sim 1$ , without changing other parameters. It is not clear what plasma characteristic would establish a species-dependent  $\eta$ , a circumstance that contrasts the inference of  $\eta(H^+) \approx \eta(He^{++})$  in the 91097 event analyzed by Baring et al. (1997).

An instructive diagnostic on the acceleration model is to probe the spatial scale of diffusion. This is performed by examining upstream distributions of high energy particles. In their 1994 paper, Gloeckler et al. discussed an energy-

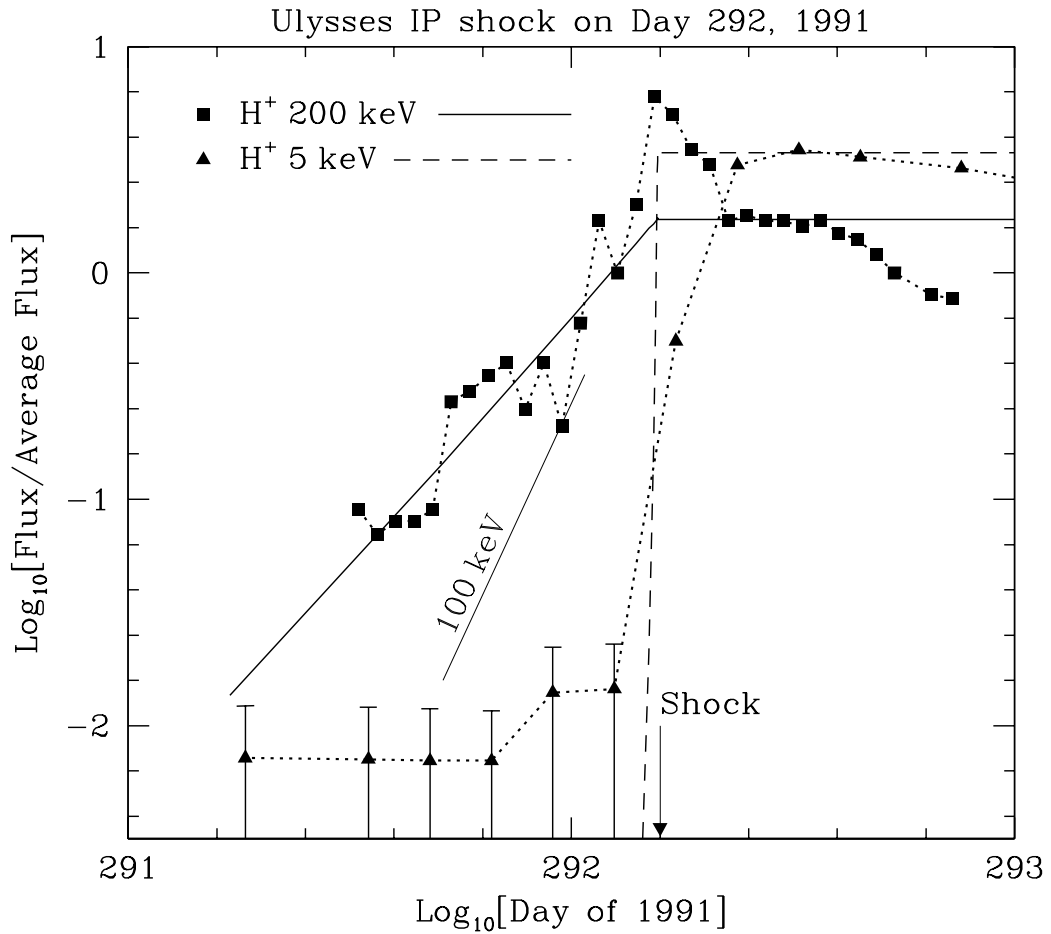


Fig. 2. The flux variations of accelerated pick-up ion populations as a function of time near the shock of Day 292, 1991. The data for 5 keV and 200 keV pick-up  $H^+$  are depicted by filled triangles and squares, respectively, and are taken from Gloeckler et al. (1994). The Monte Carlo model generated fluxes at different distances normal to the shock, and were converted to spacecraft times by incorporating solar wind convection. The 5 keV and 200 keV pick-up  $H^+$  traces are displayed as dashed and solid curves, respectively, and exhibit an exponential decline upstream of the shock that is characteristic of diffusive shock acceleration. The model normalization protocol is discussed in the text. The lightweight line labelled “100 keV” is an approximate indication of a model prediction for the expected flux variation upstream for 100 keV protons.

dependent rise in fluxes of non-thermal particles *prior* to the shock crossing. This was cited as indicating the existence of a pre-acceleration mechanism. The Monte Carlo simulation was run with flux measurement planes placed upstream of the shock at different distances, as well as downstream. This enabled determination of the number fluxes of a particular energy ion at different positions upstream of the shock. This was converted to observer’s times using the approximate speed of the Ulysses spacecraft in the solar wind. Re-

sults for two different  $H^+$  ion energies are displayed in Fig. 2, together with corresponding data from Fig. 3 of Gloeckler et al. (1994) for identical energy windows.  $H^+$  was chosen by Gloeckler et al. since good spatial resolution at 5 keV was possible. Observe that the y-axis in Fig. 2 represents ratios of flux to time-averaged flux at the respective energies, so that the normalization does not explicitly exhibit the property that the absolute flux at 200 keV is always much less than that at 5 keV when downstream of the shock. Note also that the Ulysses data normalization was established by averaging over 3 days of accumulated data, whereas the model normalization was adjusted to match observed fluxes around 1/2 day downstream of the shock.

The essential result of this comparison is that the spatial scale of the exponential decline of ions upstream of the shock is more or less identical to that of the model, for our choice of  $\eta = 5.5$ . Theoretically, high energy particles with a mean free path according to Eq. (1) establish an exponential dilution in space/time due to random scattering of the particles seeding upstream leakage against a convective flow. From standard diffusion-convection theory, the spatial scale for this dilution is  $(\kappa_{\parallel} \cos^2 \theta_{Bn1} + \kappa_{\perp} \sin^2 \theta_{Bn1})/u_{1,x}$  for a shock of obliquity  $\theta_{Bn1}$ , where  $\kappa_{\parallel} = \lambda v/3$  is the component of the spatial diffusion coefficient along the mean field,  $\kappa_{\perp} = \kappa_{\parallel}/(1 + \eta^2)$ , and  $\lambda$  is prescribed by Eq. (1). Hence, this upstream dilution scale is proportional to the proton's energy. For the 200 keV ions, the simulation results are clearly well correlated with the data prior to the shock, modulo plasma fluctuations. On the other hand, for the lower energy 5keV ions, the exponential decay has a very short time scale, a factor of 40 smaller than for the 200 keV ions, and drops to background levels very quickly. So, although the simulation results are consistent with the observed results, it is impossible to draw more definitive conclusions without an improvement in data time resolution. The 200 keV ions, however, have much longer mean free paths and travel much farther upstream, and are well correlated.

#### 4 Conclusions

The comparison of phase space distributions from the Monte Carlo simulation of diffusive shock acceleration with those observed by SWICS and HI-SCALE in the Day 292, 1991 event reveals a good deal of consistency between theory and experiment for both the proton and  $He^+$  spectra above speeds around 600 km/sec. At these speeds, the injection of pick-up protons dominates that of solar wind protons, and the acceleration of solar wind  $He^{++}$  is inefficient relative to that of pick-up  $He^+$ . The characteristic of the shock most relevant for these high energy components is its compression ratio  $r$ : to match the observed steep spectra,  $r \sim 2.1$  is required, on the low end of the range quoted by Gloeckler et al. (1994).

The normalization of the energetic ion power-laws is best fit with a model “turbulence” parameter  $\eta = 5.5 \pm 1.5$ , where  $\lambda = \eta r_g$ , corresponding to a ratio  $\kappa_\perp/\kappa_\parallel \approx 0.03$  of components of the spatial diffusion tensor. For such values, cross-field diffusion is insufficient for the Monte Carlo model to account for observed accelerated  $He^{++}$ , which requires  $\eta \sim 1$  so that the Bohm limit  $\kappa_\perp \sim \kappa_\parallel$  is approximately realized. While the high energy protons and  $He^+$  are modeled fairly well, there are significant discrepancies in the high velocity wings of the thermal protons. These deviations are slightly more marked than those found by Baring et al. (1997) in IP shocks without significant pick-up ion components. Clearly some non-diffusive element of heating may be present in the plasma shock that is not incorporated in the simulation. To explore such possibilities, it is planned to incorporate cross-shock and shock layer charge separation potentials in the Monte Carlo code in future extensions, to effect a more accurate modeling of the shock structure. It must be noted, though, that uncertainties in the shock parameters significantly impact inferences of discrepancies between theory and experiment.

The flux increases of energetic protons seen upstream of the shock are quite consistent with the expected upstream leakage associated with diffusive shock acceleration. The value of  $\eta = 5.5$  inferred from the spectral fit scales the upstream diffusive lengthscale, and the accompanying exponential decline in predicted flux is commensurate with the Ulysses data presented in Gloeckler et al. (1994). Hence, the observed upstream flux precursor is not clear evidence of a pre-acceleration mechanism, as claimed by Gloeckler et al., though it is quite possible that some pre-acceleration mechanism may be acting. A most enticing feature of this work is that a single model parameter can couple injection efficiency to the spatial scales of ions upstream of the shock. Whether or not this identifies diffusion as the dominant operating mechanism remains to be seen, but it is clear that processes acting on the scales of a few gyroradii control both injection and upstream transport in this interplanetary shock.

## 5 References

- Balogh, A., Forsyth, R. J., Ahuja, A., et al. The interplanetary magnetic field from 1 to 5 AU - ULYSSES observations. *Adv. Space Res.* 13, (6) 15–24. 1993.
- Balogh, A., González-Esparza, J. A., Forsyth, R. J., et al. Interplanetary Shock Waves: ULYSSES Observations In and Out of the Ecliptic Plane. *Space Sci. Rev.* 72, 171–180. 1995.
- Baring, M. G., Ellison, D. C. & Jones, F. C. Monte Carlo simulations of particle acceleration at oblique shocks. *ApJ Supp.* 90, 547–552. 1994.
- Baring, M. G., Ogilvie, K. W., Ellison, D. C., & Forsyth, R. J. Acceleration of Solar Wind Ions by Nearby Interplanetary Shocks: Comparison of Monte Carlo Simulations with Ulysses Observations. *ApJ* 476, 889–902. 1997.

- Bell, A. R. The acceleration of cosmic rays in shock fronts. I. M.N.R.A.S. 182, 147–156. 1978.
- Bieber, J. W., Matthaeus, W. H., Smith, C. W., et al. Proton and electron mean free paths: The Palmer consensus revisited. ApJ 420, 294–306. 1994.
- Burgess, D. Alpha particles in field-aligned beams upstream of the bow shock - Simulations. Geophys. Res. Lett. 16, 163–166. 1989.
- Burton, M. E., Smith, E. J., Goldstein, B. E., et al. ULYSSES - Interplanetary shocks between 1 and 4 AU. Geophys. Res. Lett. 19, 1,287–1,289. 1992.
- Decker, R. B., Pesses, M. E., & Krimigis, S. M. Shock-associated low-energy ion enhancements observed by Voyagers 1 and 2. J. Geophys. Res. 86, 8,819–8,831. 1981.
- Ellison, D. C., Baring, M. G., & Jones, F. C. Acceleration Rates and Injection Efficiencies in Oblique Shocks. ApJ 453, 873–882. 1995.
- Ellison, D. C., Baring, M. G. & Jones, F. C. Nonlinear Particle Acceleration in Oblique Shocks. ApJ 473, 1,029–1,050. 1996.
- Ellison, D. C., Giacalone, J., Burgess, D., & Schwartz, S. J. Simulations of particle acceleration in parallel shocks: Direct comparison between Monte Carlo and one-dimensional hybrid codes. J. Geophys. Res. 98, 21,085–21,093. 1993.
- Ellison, D. C., Jones, F. C. & Baring, M. G. Direct Acceleration of Pickup Ions at the Solar Wind Termination Shock: The Production of Anomalous Cosmic Rays. ApJ 512, 403–416. 1999.
- Ellison, D. C., Jones, F. C. & Eichler, D. Monte Carlo simulation of collisionless shocks showing preferential acceleration of high A/Z particles. J. Geophys. - Zeitschrift fuer Geophysik 50, 110–113. 1981.
- Ellison, D. C., Jones, F. C. & Reynolds, S. P. First-order Fermi particle acceleration by relativistic shocks. ApJ 360, 702–714. 1990.
- Ellison, D. C., Möbius, E., & Paschmann, G. Particle injection and acceleration at earth's bow shock - Comparison of upstream and downstream events. ApJ 352, 376–394. 1990.
- Forman, M. A., Jokipii, J. R. & Owens, A. J. Cosmic-Ray Streaming Perpendicular to the Mean Magnetic Field. ApJ 192, 535–540. 1974.
- Giacalone, J., Burgess, D., & Schwartz, S. J. Ion acceleration at parallel shocks: Self-consistent plasma simulations, in ESA, Study of the Solar-Terrestrial System, 65–70. 1992.
- Giacalone, J., Burgess, D., Schwartz, S. J. & Ellison, D. C. Ion injection and acceleration at parallel shocks - Comparisons of self-consistent plasma simulations with existing theories. ApJ 402, 550–559. 1993.
- Giacalone, J. & Jokipii, J. R. The Transport of Cosmic Rays across a Turbulent Magnetic Field. ApJ 520, 204–214. 1999.
- Gloeckler, G., Geiss, J., Roelof, E. C., et al. Acceleration of interstellar pickup ions in the disturbed solar wind observed on ULYSSES. J. Geophys. Res. 99, 17,637–17,643. 1994.

- González-Esparza, J. A., Balogh, A., Forsyth, R. J., et al. Interplanetary shock waves and large-scale structures: Ulysses' observations in and out of the ecliptic plane. *J. Geophys. Res.* 101, 17,057–17,072. 1996.
- Gosling, J. T., Asbridge, J. R., Bame, S. J., et al. Interplanetary ions during an energetic storm particle event - The distribution function from solar wind thermal energies to 1.6 MeV. *J. Geophys. Res.* 86, 547–554. 1981.
- Gosling, J. T., Thomsen, M. F., Bame, S. J., & Russell, C. T. On the source of diffuse, suprathermal ions observed in the vicinity of the earth's bow shock. *J. Geophys. Res.* 94, 3,555–3,563. 1989.
- Hoang, S., Lacombe, C., Mangeney, A., et al. Interplanetary shocks observed by ULYSSES in the ecliptic plane as a function of the heliocentric distance. *Adv. Space Res.* 15 (8/9), 371–374. 1995.
- Hoppe, M. M., Russell, C. T., Frank, L. A., et al. Upstream hydromagnetic waves and their association with backstreaming ion populations - ISEE 1 and 2 observations. *J. Geophys. Res.* 86, 4,471–4,492. 1981.
- Jokipii, J. R. & Coleman, P. J. Cosmic-Ray Diffusion Tensor and Its Variation Observed with Mariner 4. *J. Geophys. Res.* 73, 5,495–5,501. 1968.
- Jones, F. C., Birmingham, T. J., & Kaiser, T. B. Partially averaged field approach to cosmic ray diffusion. *Phys. Fluids* 21, 347–360. 1978.
- Jones, F. C. and Ellison, D. C. The plasma physics of shock acceleration. *Space Sci. Rev.* 58, 259–346. 1991.
- Kang, H., & Jones, T. W. Diffusive Shock Acceleration Simulations: Comparison with Particle Methods and Bow Shock Measurements. *ApJ* 447, 944–961. 1995.
- Kang, H., & Jones, T. W. Diffusive Shock Acceleration in Oblique Magnetohydrodynamic Shock: Comparison with Monte Carlo Methods and Observations. *ApJ* 476, 875–888. 1997.
- Kucharek, H. & Scholer, M. Injection and acceleration of interstellar pickup ions at the heliospheric termination shock. *J. Geophys. Res.* 100, 1,745–1,754. 1995.
- Kulsrud, R. & Pierce, W. P. The Effect of Wave-Particle Interactions on the Propagation of Cosmic Rays. *ApJ* 156, 445–469. 1969.
- le Roux, J. A., Potgieter, M. S., & Ptuskin, V. S. A transport model for the diffusive shock acceleration and modulation of anomalous cosmic rays in the heliosphere. *J. Geophys. Res.* 101, 4,791–4,804. 1996.
- Liewer, P. C., Goldstein, B. E., & Omidi, N. Hybrid simulations of the effects of interstellar pickup hydrogen on the solar wind termination shock. *J. Geophys. Res.* 98, 15,211–15,220. 1993.
- Mason, G. M., Gloeckler, G., & Hovestadt, D. Temporal variations of nucleon abundances in solar flare energetic particle events. I - Well-connected events. *ApJ* 267, 844–862. 1983.
- Möbius, E., Scholer, M., Sckopke, N., et al. The distribution function of diffuse ions and the magnetic field power spectrum upstream of earth's bow shock. *Geophys. Res. Lett.* 14, 681–684. 1987.

- Quest, K. B. Theory and simulation of collisionless parallel shocks. *J. Geophys. Res.* 93, 9,649–9,680. 1988.
- Sarris, E. T., & Van Allen, J. A. Effects of interplanetary shock waves on energetic charged particles. *J. Geophys. Res.* 79, 4,157–4,173. 1974.
- Scholer, M., Hovestadt, D., Ipavich, F. M., & Gloeckler, G. Conditions for acceleration of energetic ions greater than 30 keV associated with the earth's bow shock. *J. Geophys. Res.* 85, 4,602–4,606. 1980.
- Tan, L. C., Mason, G. M., Gloeckler, G., & Ipavich, F. M. Downstream energetic proton and alpha particles during quasi-parallel interplanetary shock events. *J. Geophys. Res.* 93, 7,225–7,243. 1988.
- Trattner, K. J., & Scholer, M. Diffuse alpha particles upstream of simulated quasi-parallel supercritical collisionless shocks. *Geophys. Res. Lett.* 18, 1,817–1,820. 1991.
- Vasyliunas, V. M., & Siscoe, G. L. On the flux and the energy spectrum of interstellar ions in the solar system. *J. Geophys. Res.* 81, 1,247–1,252. 1976.
- Winske, D., Thomas, V. A., Omidi, N., & Quest, K. B. Re-forming supercritical quasi-parallel shocks. II - Mechanism for wave generation and front re-formation. *J. Geophys. Res.* 95, 18,821–18,832. 1990.